

Cilt Kanseri Görüntülerinde FCN8-ResNetC ve Görüntü İşleme ile Kıl Temizliği ve Lezyon Bölütleme

Araştırma Makalesi/Research Article

 Cihan AKYEL¹,  Nursal ARICI²

¹ Graduate School of Informatics, Management Information Systems, Gazi University, Ankara, Turkey

² Management Information Systems Department, Applied Sciences Faculty, Gazi University, Ankara, Turkey

cihan.akyel1@gazi.edu.tr, nursals@gazi.edu.tr

(Geliş/Received:19.01.2022; Kabul/Accepted:18.04.2022)

DOI: 10.17671/gazibtd.1060330

Özet—Cilt kanseri oldukça yaygın görülmektedir. Cilt kanseri tedavisinde erken tespit önemlidir. Artık cilt kanseri tanısında bilgisayar teknolojisi temelli yöntemler (derin öğrenme, görüntü işleme) daha yaygın olarak kullanılmaktadır. Bu yöntemler ile tanı sürecinde insan hatası ortadan kaldırılabilir. Lezyon görüntüleri üzerindeki kıl gürültüsünün temizlenmesi doğru bölütleme için önem teşkil eder. Doğru bölütlenmiş lezyon görüntüsü ile cilt kanseri tanısında başarı oranı artacaktır. Bu çalışma, cilt kanseri görüntülerinde kıl temizliği ve bölütleme için FCN8 tabanlı yeni bir yaklaşım sunmaktadır. FCN8 algoritmasına ResNetC eklenerek başarı artışı sağlanmıştır. ResNetC ResNet tabanlı yeni bir modeldir. Çalışmada ISIC 2018'e ait iki veri seti ve PH2 veri seti kullanıldı. Kıl temizliğinde eğitim başarısı %89.380, lezyon bölütlemesinde ise %97.050 olarak elde edildi. Lezyon görüntülerindeki kıl gürültüsü temizliği için 3000 kıl maskesi çalışmada kapsamında oluşturulmuştur.

Anahtar Kelimeler—derin öğrenme, kıl temizliği, cilt kanseri, FCN, ResNet

Hair Removal and Lesion Segmentation with FCN8-ResNetC and Image Processing in Images of Skin Cancer

Abstract— Skin cancer is quite common. Early detection is crucial for the treatment of skin cancer. Methods based on computer technology (deep learning, image processing) are now increasingly used to diagnose skin cancer. These methods can eliminate human error in the diagnostic process. Removing hair noise from lesion images is essential for accurate segmentation. A correctly segmented lesion image increases the success rate in diagnosing skin cancer. In this study, a new FCN8-based approach for hair removal and segmentation in skin cancer images is presented. Higher success was achieved by adding ResNetC to FCN8. ResNetC is a new model based on ResNet. Two datasets were used for the study: ISIC 2018 and PH2. Training success was 89.380% for hair removal and 97.050% for lesion segmentation. 3000 hair masks were created as part of the study to remove hair noise in the lesion images.

Keywords—deep learning, hair removal, skin cancer, FCN, ResNet

1. INTRODUCTION

Cancer is the uncontrolled proliferation of cells in various organs [1]. Cancer is a deadly disease. In 2020, ten million people died from cancer [2]. This is a very high rate for other reasons as well. Skin cancer is quite common among different types of cancer in the world.

Nowadays, the number of cases has increased rapidly due to the influence of environmental conditions such as sunlight. In skin cancer, there are melanoma, basal cell

carcinoma, squamous cell carcinoma and actinic keratosis. Melanoma is the most deadly skin cancer. The number of new cases of melanoma in the US in 2021 is 115320 and the number of deaths is 11540, and 63% of deaths from skin cancer are malignant [3].

Early diagnosis is critical for the treatment of skin cancer. The five-year survival rate is 92% [4]. Melanoma-type skin cancer tends to metastasize and spread to other tissues. The likelihood of metastasis is high for melanoma tumors with a penetration depth greater than 2 mm [5].

Traditional methods such as the ABCD rule, biopsy, and dermoscopy are used in skin cancer diagnosis. The ABCDE rule is a standard method (A: asymmetry, B: margin, C: color, D: diameter). Dermatologists can predict melanoma with 75% accuracy, which is low [6]. Moreover, this diagnostic method is influenced by the person's current situation. Dermatologists evaluate dermoscopy images to predict skin cancer. This method can take a lot of time. And human-caused errors may occur in this process [7]. In this traditional method, the diagnosis of skin cancer takes a long time. For this reason, patient comfort may be affected. The accuracy of cancer detection in visual inspection may decrease depending on the dermatologist's qualification. Considering the importance of early diagnosis of skin cancer, it becomes clear how important the situation is. The success rate of the best dermatologists is about 80%. And this rate depends on human factors [8]. At this point, the importance of the new method becomes clear.

Nowadays, novel approaches are frequently used to diagnose skin cancer [9]. Artificial intelligence and image processing are new methods for diagnosing skin cancer. Surgical techniques take a lot of time and disturb patients. Computerized algorithms can eliminate human errors and achieve successful results as an expert. When detecting skin cancer, it is crucial to remove hair-like noise from the lesion. These methods have some advantages. There are no human errors in this method. And they require very little time. But this method also has some challenges. Correct removal of hair in lesion images is a major challenge. Hair removal affects the accurate segmentation of the lesions. This improves the accuracy [10].

Many deep learning models such as FCN8, FCN16, FCN32, UNet, LinkNet and ResNet. Image processing is essential for preparing data for Deep Learning algorithms. It is seen that image processing features such as color spaces (e.g., YUV, RGB, HSV), pixel values, features, edge detection, thresholding, and contrast enhancement are used in such studies [11, 12].

1.1. Related Works

Image processing is often used to remove noise. DullRazor is an image processing algorithm. And it is used to remove hair noise in skin cancer images. This method is not very effective. But it is easy to use. For this reason, this algorithm is widely used now. This algorithm cleans up hair in the lesion based on the pixel values of the images [13].

In some studies, image processing is used to remove hair noise from lesion images without Deep Learning. In these studies, contrast and brightness in the images are critical for these operations. In these methods, the noise is removed based on the difference of pixel properties inside and outside the noise [14].

In the study by Zafar et al, correct lesion segmentation was aimed by using U-Net and ResNet architectures together. Using different models together increases

accuracy. They used image modification with the estimated mask to remove hair noise. The disadvantage of this method is that the process can affect areas of the lesion other than hair. The hair noise is removed based on the pixel values of the clean areas of the lesions. This study shows that FCN has higher accuracy than U-Net [15].

Another critical step after hair removal is the correct segmentation of the lesion. The main problem is that a valid threshold procedure for each lesion is impossible. It is impossible to accurately locate and segment the edges of the lesion if the threshold is inaccurate. In this context, Celebi et al. presented an unsupervised, fast and successful algorithm for lesion edge detection and accurate segmentation [16].

In the literature, some studies use pre-trained models such as VGG16 and efficiennet. With these pre-trained models, the accuracy improves and the number of epochs decreases. In one study, U-Net with VGG 16 encoder was used. They achieved a dice accuracy of 91.5% with the ISIC 2017 dataset. There was no hair removal stage in this study [17]. Akyel and Arıcı proposed a U-Net-based model. They achieved about 88% in noise removal and 92% in segmentation using the ISIC 2018 dataset. This study only includes images with hair noise [18].

A model is proposed in one study. It is shown that DullRazor is not sufficient to remove hair noise in this study. The dice accuracy was calculated to be 88.43%. They mentioned that hair removal increases the accuracy [19]. Rajan et al. proposed a segNet-based model. In this study, a dice accuracy of 85.16% was obtained using the PH2 dataset. These values can be improved by various hair removal methods [20]. In one study, a hair dataset was created. This dataset contains only simulated noise. The model was used at 512x512, which is high [21]. Alex et al. presented a U-Net based method for hair cleaning. In this study, a hair dataset was created. The archived about 96% dice coefficient in hair removal and about 86% in segmentation [22]. Polat et al. presented a new method. They used histograms and clusters. In this study, 1279 images were used [23]. A study worth mentioning in this area is the work of Sahiner et al. First, the images are processed by converting them to gray scale and using median filters and histogram values. Then, the segmentation process is performed by determining the corners and the area of the lesion based on the pixel values. In the third part, the results of this project were compared with our results [24]. Hasan et al. presented a new and automated semantic network method for skin cancer segmentation. In this study, U-Net and FCN algorithms are applied together and the results are compared. As a result of the study, a success rate of about 87% was obtained. The ISIC 2017 dataset was used in the study. This study shows that the pixel properties affect the accuracy. The results of lesion segmentation were affected by low contrast. As can be seen, one of the major problems in lesion segmentation is brightness, contrast transitions, and color conditions [25].

In another study, success of about 70% was achieved. Segmentation is performed by image processing without hair removal. The effect of this situation on the low success rate cannot be ignored [26]. Cihan and Arıcı presented a model called LinkNet-B7. They created a noise dataset that includes hair, ink marks etc. In this study, lesion segmentation phase was performed with cleaned images [27].

Examining the literature, Deep Learning and image processing methods are not alone in hair removal and segmentation. In this study, these two approaches were combined. We expect that it will contribute to the literature with this aspect. We created a hair dataset containing only hair noises. The second section explains the material and the method we used to test the proposed approaches. The results of the method are presented, discussed and summarized in the third section.

2. MATERIAL AND METHOD

2.1. Material

We used two ISIC2018 datasets. The first dataset contains 10015 RGB images in jpeg format in the first dataset. From this dataset, 2000 images containing hair noise (they may also have other noise) were randomly selected and increased to 8000 by data augmentation at the hair removal stage. This dataset is now called the cleaning dataset (8000 RGB images and masks created in the hair removal stage) [28]. The cleaning dataset can be seen in Figure 1. A hardware system with a GTX3080 graphics card and 24 GB of DDR5 RAM was used in multiple stages.

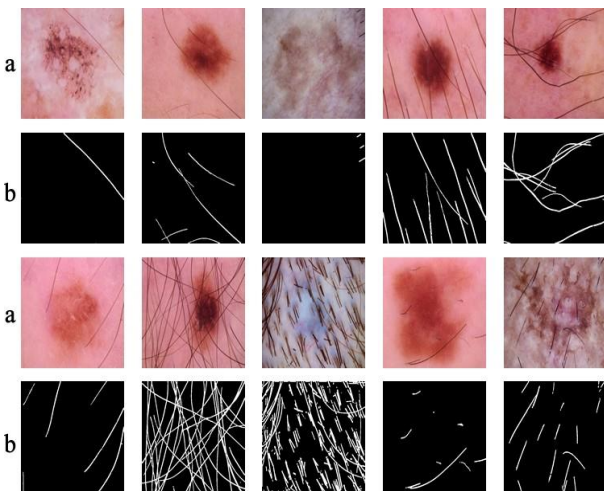


Fig. 1. Cleaning dataset

The second dataset (1300 images and masks) [29] and 200 images belonging to PH2 [30] were used for lesion segmentation. We increased the number of images to 52800 by data augmentation. This dataset will be referred to as the segmentation dataset in the following.

In both stages, data augmentation was used to increase learning accuracy and prevent the system from falling into overfitting (90 and 180 degree rotation, horizontal and

vertical mirroring). The segmentation data set can be seen in Figure 2.

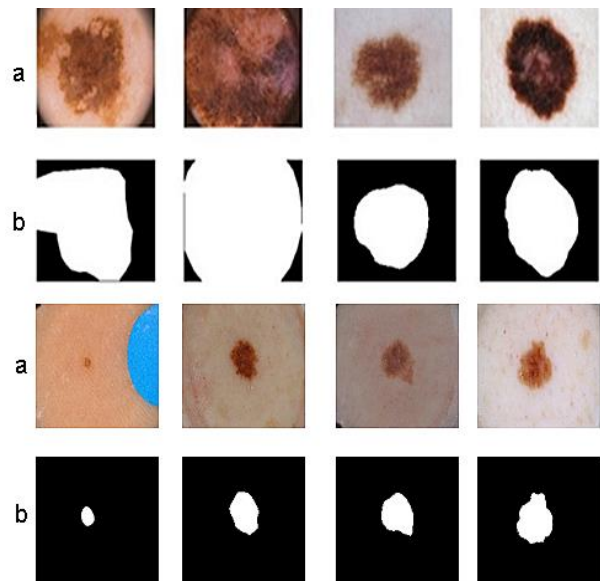


Fig. 2. Segmentation dataset

2.1.1. Image Preprocessing

In both stages, data augmentation was used. Parameters for ImageDataGenerator:

- horizontal_flip=True
- vertical_flip=True,
- width_shift_range=0.1,
- height_shift_range=0.1

The images were divided into data sets of 16 slices (224x224x3). So we can use a total of 896x896x3 image sizes as inputs. This helps to improve the accuracy. The cleaning dataset consists of 128000 images and the segmentation dataset consists of 844800 images. Figure 3 illustrates this process.

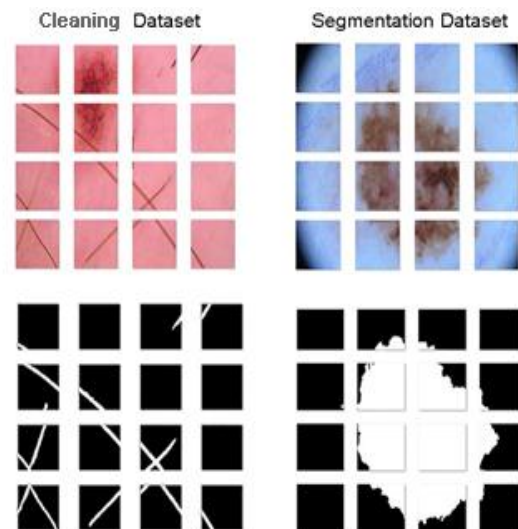


Fig. 3. Image slices

2.2. Method

We divided the data set into 70% training, 20% validation, and 10% testing. In our study, the system was trained at these rates in the training stage, and no overfitting occurred. For this reason, the rates given for the training and test data were used.

FCN was chosen for the training stages. Training accuracy can be increased using other deep learning methods such as U-Net and LinkNet.

2.2.1. Proposed Model

We used the FCN8 algorithm. The FCN8 algorithm has 27 layers, imagenet weights, and an input size (224x224). The optimizer was determined to be adam. We used the dice coefficient and the softmax loss function. The general architecture of FCN is shown in Figure 4.

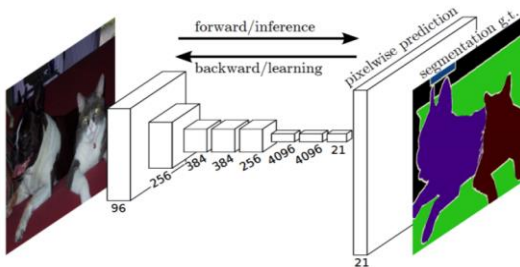


Fig. 4. FCN model [25].

Each data layer in a Convnet (Convolutional Neural Network) is a three-dimensional array of size $h \times w \times d$ (h and w are spatial dimensions and d is the feature or channel dimension). The first layer is the image, with pixel size $h \times w$ and d color channels. Convnets are built on translation invariance. The basic components: Convolution, Pooling and Activation functions operate on local input regions and depend only on the relative spatial coordinates. FCN uses 1×1 convolutional layers [31]. We used the softmax output function, which is used in FCN algorithms.

We proposed a new ResNet model. And we inserted it into FCN8 algorithm before the last layer. The new ResNet model is called ResNetC. Figure 5 shows the architecture of ResNetC. This model provides about 1% more success than the basic ResNet model.

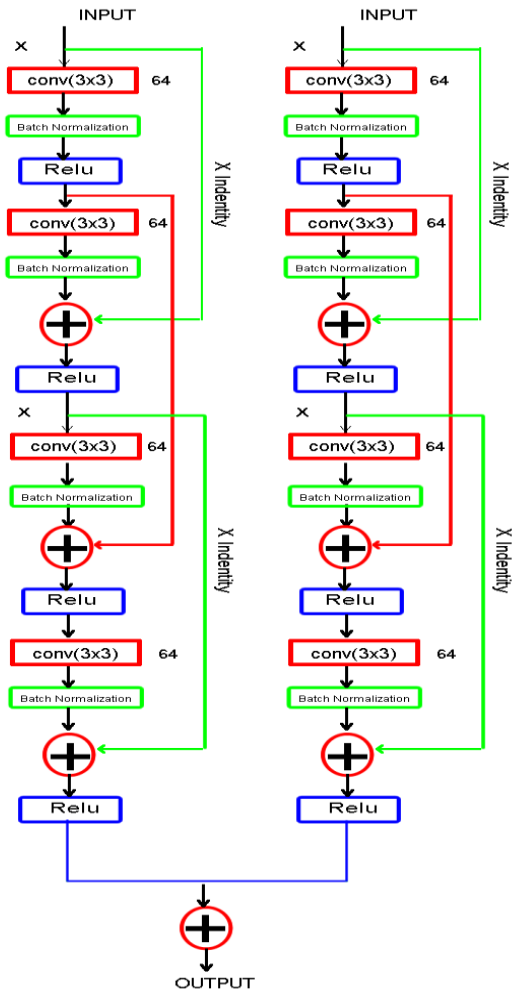


Fig. 5. ResNetC Architecture.

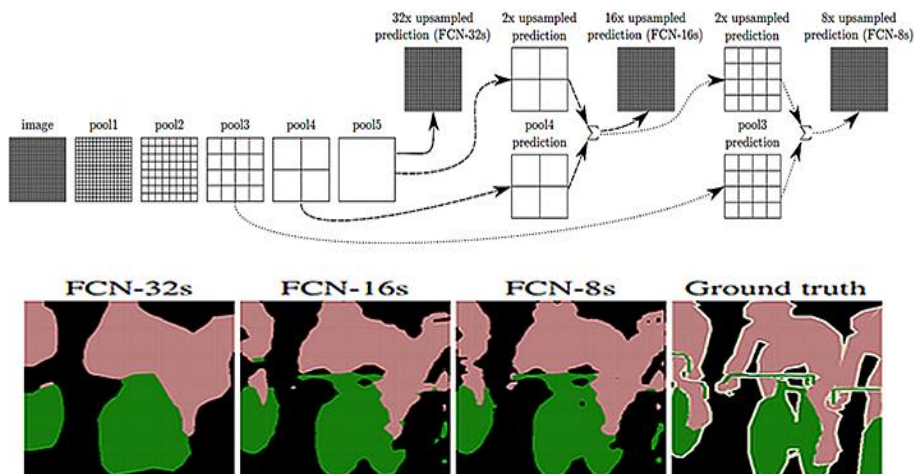


Fig. 6. Comparison of FCN8, 16, 32 [30]

FCN8 includes an upsampling operation. Additional predictions of pool3 at Stride 8, providing even more precise bounds. In FCN8, an 8-fold upsampling is used. This means that each pixel value is multiplied by 8 to equalize the size of the input and output images. FCN8 has more features with pool three than FCN16, 32, so it achieves the best results. This can be seen in Figure 6 [31]. The parameters used in the training stages are listed in Table 1.

Table 1. Model Parameters

| Parameters | Hair Removal Stage | Lesion Segmentation Step |
|---------------|--------------------|--------------------------|
| Batch Size | 8 | 8 |
| Learning Rate | 0.01 | 0.01 |
| Epoch Number | 1000 | 1000 |
| Input Size | 224*224 | 224*224 |
| Optimizer | Adam | Adam |

2.2.2. Parameters

• **Dice coefficient:** The dice coefficient is $2 * \text{the overlap area} / \text{total number of pixels in both images}$ (ground truth: Y, predicted segmentation: X) [32].

$$(2 * |X \cap Y|) / (|X| + |Y|) \quad (1)$$

• **The Jaccard:** Jaccard similarity index is the most pronounced relationship between the intersection and union of the segmented image and the ground truth [32].

• **Loss function:** We use the softmax loss function for both levels. Softmax loss is a softmax activation plus a cross-entropy loss. The cross-entropy loss is the sum of the negative logarithms of the probabilities [33].

• **Optimizer:** Adam optimization is a stochastic gradient descent method [34].

• **mIoU(Mean Intersection Over Union):** Given an image, the IoU measure gives the similarity between the predicted region and the true region for an object present in the image and is defined as the size of the intersection divided by the union of the two regions [35].

• We used mean IoU in Keras library. In this study, mean IoU was used.

The format of an equation should be like TP: True Positive, FP: False Positive, and FN: False Negative.

$$IoU = \frac{TP}{FP+TP+FN} \quad (2)$$

2.3. First Stage: Hair Removal Stage

The hair masks of the images in the cleaned dataset were created at this stage and the FCN8 was trained with these images and masks. The hair removal algorithm includes the following steps.

Step 1: The images were resized to 224x224x3 (2000 RGB images in total).

Step 2: The hair masks of the images were created by Adaptive Thresholding.

Step 3: In this step, tiny bubbles and fine hairs were removed from the image using the median filter. Then opening and closing operations were performed to remove the noise in the hair masks.

Step 4: Hair masks created in the first three steps were corrected by examining the hair noise in the lesion using the Adobe Fireworks program (Figure 7).

A total of 2000 hair masks were created in this step. With data augmentation, the number of images and masks then increased to 8000.

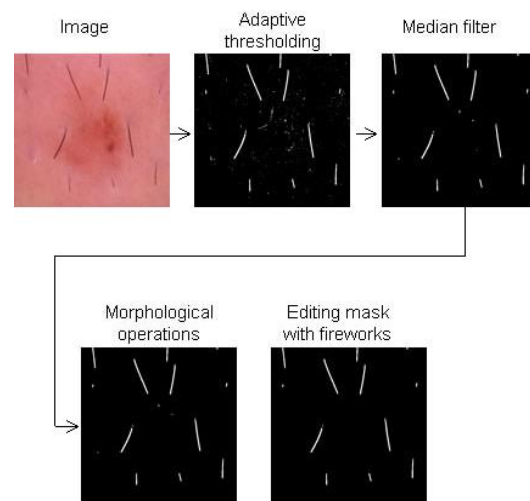


Fig. 7. Adaptive threshold process.

Step 5: The cleaned datasets are divided into 89600 training, 25600 validation and 12800 test datasets.

Step 6: The model was trained for 1000 epochs.

Step 7: The model was created with test data. The masks were cleaned using morphological operations and a median filter. Using a mask that predicts hair noise, the image was cleaned using INPAINT. At this stage, the INPAINT function in the OpenCV library was used.

2.4. Second Stage: Lesion Segmentation Stage

The system was trained with the FCN8 algorithm at this stage. A segmentation dataset consisting of 844800 images and masks was used for this purpose. Noise in the images was removed in the first stage. Images containing different noises, such as patches, were not excluded from the dataset. The lesion segmentation algorithm includes the following steps.

Step 1: Using the model obtained in the previous step, the dataset was cleaned of hair noise. And the images and masks were reduced to 224x224x3 channels (RGB images).

Step 2: In this step, the number of images was increased to 52800 by data augmentation.

Step 3: The segmentation datasets are divided into 591360 training, 168960 validation and 84480 test datasets.

Step 4: The model was trained for 1000 epochs.

Step 5: Cleaning the segmentation results from noise using morphological operations (Median Filter, Open, Close, Dilate).

The mask estimated in this step was optimized by image processing. Noise was removed on the mask using the median filter. Later, the opening and closing operations were applied and the noise in the segmentation was cleaned. Dilatation function was used to correct area reductions caused by previous operations. And tiny regions were removed. In this way, the images of the lesions can be segmented more accurately.

3. RESULTS

In this study, the FCN8 hair removal and lesion segmentation algorithm achieved validation accuracies of approximately 88.510% and 94.200% with the specified parameters. The algorithm was run for 1000 epochs for two steps (hair removal and lesion segmentation).

Since there was no significant decrease in the validation loss rate after 1000 epochs, the training was stopped with this number of epochs. The results can be seen in Tables 2 and 3.

Table 2. Hair removal stage results

| Hair Removal Stage | | | | |
|-------------------------|--------------|--------|--------|--------|
| Parameters | FCN8-ResNetC | FCN8 | FCN16 | FCN32 |
| Training Accuracy (%) | 90.300 | 89.380 | 87.600 | 85.150 |
| Training Loss(%) | 11.950 | 12.020 | 13.950 | 15.200 |
| Validation Accuracy (%) | 89.600 | 88.540 | 85.320 | 84.700 |
| Validation Loss(%) | 7.285 | 7.350 | 7.800 | 8.750 |
| Jac(%) | 85.900 | 85.050 | 83.200 | 81.100 |
| mIoU(%) | 89.050 | 88.250 | 85.300 | 83.950 |
| Sensitivity | 89 | 88.100 | 87.150 | 85.300 |
| Specificity | 90.400 | 89.600 | 87.900 | 84.860 |

Figures 8 and 9 show the results of hair removal and lesion segmentation.

During the literature review, it was found that thresholding and image processing algorithms have been used in many hair removal studies. The common problem in these studies is that the hair mask cannot be estimated correctly and there is loss of data due to hair removal. Hair noise affects the accuracy of lesion segmentation. Figure 10 shows that success decreases when the mask is calculated with the model without hair removal.

Table 3. Lesion segmentation stage results

| Lesion Segmentation Stage | | | | |
|---------------------------|--------------|--------|--------|--------|
| Parameters | FCN8-ResNetC | FCN8 | FCN16 | FCN32 |
| Training Accuracy (%) | 98 | 97.05 | 95.100 | 91.050 |
| Training Loss(%) | 9.200 | 9.880 | 10.220 | 11.300 |
| Validation Accuracy (%) | 95.100 | 94.440 | 91.200 | 89.600 |
| Validation Loss(%) | 5.600 | 5.920 | 6.600 | 6.750 |
| Jac(%) | 92.200 | 91.700 | 85.950 | 85.800 |
| mIoU(%) | 93.100 | 92.360 | 89.320 | 87.300 |
| Sensitivity | 97.500 | 96.800 | 94.800 | 90.700 |
| Specificity | 98.050 | 97.300 | 95.250 | 91.600 |

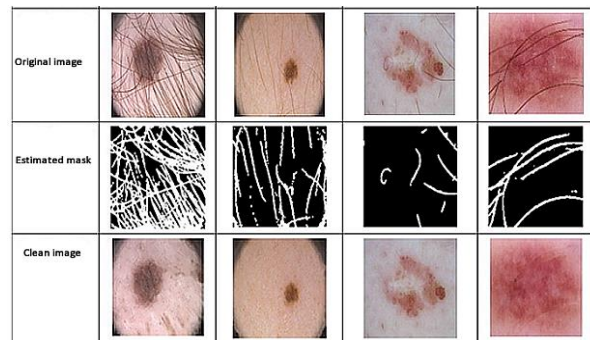


Fig. 8. Results of test data.

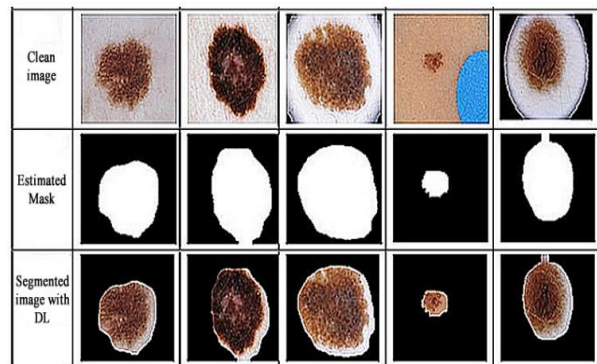


Fig. 9. Lesion segmentation results of test data.

Some studies show that FCN8 has higher accuracy than U-Net in hair removal and segmentation [15, 25]. In the 1st stage, noises are removed from the lesion. In the 2nd stage, more accurate results were obtained by re-segmentation with image processing on the noise-free image used as input.

Figure 11 shows the comparison between our model and the document [24]. In the aforementioned study, a success rate of 96% was achieved. These images are complex examples of segmentation. Since they have a low contrast transition and a locally high brightness, it can be seen that our model gives more successful results.

The study by Talavera-Marinez et al. used a hair dataset containing only simulated hair noises, similar to our work [21]. The study by Alex et al. is similar to ours. In this

study, a noise dataset was created (306 images and masks in ISIC 2018 [22]).

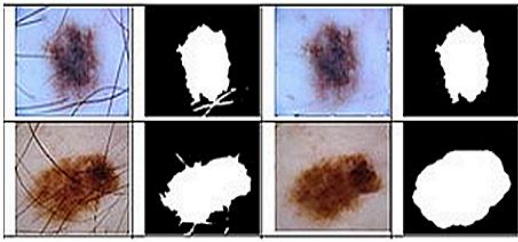


Fig. 10. The effect of hair removal.

| Model | Image number | Original image | Ground truth mask | Method result |
|-------------|--------------|----------------|-------------------|---------------|
| Other model | IMD088 | | | |
| Our model | IMD088 | | | |

Fig.11. Comparison of models.

This study compared other models with the same dataset in the segmentation stage. In addition, we selected two studies. The study by Phan et al. used a U-grid-based model [36]. And Bagheri et al. proposed an RNN-based model [37]. Tables 4 and 5 show the comparison of the results of the different models.

Table 4. Comparison of the models when trained on the PH2 dataset.

| Method | Dice Score (%) | Dataset | Image Num |
|----------------------------|----------------|------------|------------|
| Popescu and El-Khatib [14] | 86.79 | PH2 | 200 |
| Zafar et al.[15] | 92.4 | PH2 | 200 |
| Rajan et al.[20] | 85.16 | PH2 | 200 |
| Phan et al.[35] | 94 | PH2 | 200 |
| Bagheri et al. [36] | 89.83 | PH2 | 200 |
| Proposed Method | 97.10 | PH2 | 200 |

Table 5. Comparison of models when trained on ISIC datasets.

| Method | Dice Score (%) | Dataset | Image Num |
|------------------------|----------------|------------------|--------------|
| Zafar et al.[15] | 85.8 | ISIC 2017 | - |
| Thanh et al. [17] | 91.5 | ISIC 2017 | - |
| Şahin et al. [19] | 88.43 | ISBI 2016 | 900 |
| Polat et al. [23] | 93.69 | ISBI 2016 | 1279 |
| Hasan et al. [25] | 87.5 | ISIC 2017 | 2750 |
| Kalouche [26] | 70 | ISBI 2016 | 1280 |
| Proposed Method | 96.50 | ISIC 2018 | 13200 |

4. CONCLUSION

In contrast to the current literature on hair removal and segmentation stages, we presented new approaches. In the hair removal stage, we created a dataset of hair masks.

We used both Deep Learning and image processing. In this way, a better elimination of the different hair noises was achieved. It can be seen that the new approach used for hair removal gives successful results. With this dataset, the training with Deep Learning was completed.

Images with different noises, such as patches, were not excluded from the dataset. Although this resulted in a slight decrease in success rate, the sensitivity of the model increased. mIoU was 88% for hair removal and 92% for lesion segmentation. mIoU indicates the percentage of overlap between the actual and predicted mask.

In the literature, the highest resolution is generally 512x512x3. In this study, the images were divided into 16 layers (224x224x3). So, in total, we can use an image size of 896x896x3 as input. Thanks to this, no pixel values are lost. The training accuracy has increased by almost 3% due to the use of slices and data augmentation.

We have seen that some images give poor results. We have mentioned this situation in related works because they have low contrast and low brightness. In Figure 12 you can see some examples.

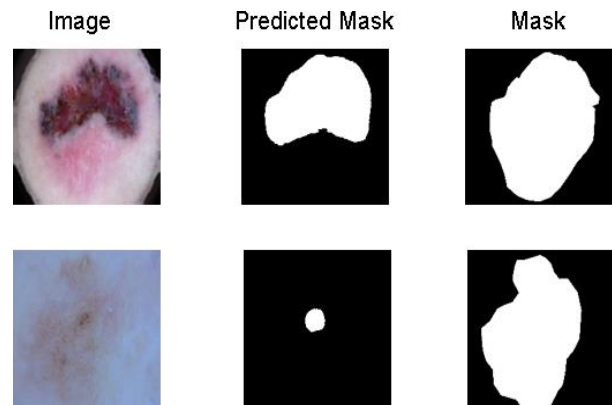


Fig.12. Examples of poor results.

REFERENCES

- [1] O. Baykara, "Current Modalities in Treatment of Cancer", *Balıkesir Health Sciences Journal*, 5(3), 154-165, 2016.
- [2] Internet: WHO, <https://www.who.int/news-room/fact-sheets/detail/cancer>, 20.10.2021.
- [3] R. L. Siegel, K.D. Miller KD, Jemal A. "Cancer statistics", *ACS Journal*, 71(1), 7-33, 2021.
- [4] H. M. Unver, E. Ayan, "Skin Lesion Segmentation in Dermoscopic Images with Combination of YOLO and GrabCut Algorithm", *Diagnostics Journal*, 9(72), 1-21, 2019.
- [5] K. H. Güngör, *Metastaz Yapmamış Melanoma Ve Melanoma Dışı Deri Kanseri İçin Geliştirilmiş Olan Deri Kanseri İlişkili Yaşam Kalitesi Ölçeğinin (Dkykö) Türkçe Geçerlilik Ve Güvenilirliğinin Araştırılması*, Tıpta Uzmanlık Tezi, Ankara Üniversitesi Tıp Fakültesi, 2016.

- [6] Internet: Ryerson University, https://rshare.library.ryerson.ca/articles/thesis/Skin_Lesion_Segmentation_Techniques_for_Melanoma_Diagnosis_Comparative_Studies/14649345/1, 18.01.2022.
- [7] Internet: Arxiv, <https://arxiv.org/ftp/arxiv/papers/1904/1904.11126.pdf>, 25.02.2021.
- [8] M. A. Kadampur, S. A. Riyae, "Skin cancer detection: Applying a deep learning-based model-driven architecture in the cloud for classifying dermal cell images", *Informatics in Medicine Unlocked Journal*, 18, 1-6, 2020.
- [9] M. Senan, M. Jadhav, "Classification of Dermoscopy Images for Early Detection of Skin Cancer – A Review", *International Journal of Computer Applications*, 178(17), 37-43, 2019.
- [10] Internet: Science Direct, <https://www.sciencedirect.com/science/article/pii/S1877050916305865>, 11.05.2021.
- [11] Z. Faisal, N. Abbadi, "New Segmentation Method for Skin Cancer Lesions", *Journal of Engineering and Applied Sciences*, 12(21), 5598-5602, 2017.
- [12] S. Jain, V. Jagtap, N. Pise, "Computer-aided Melanoma skin cancer detection using Image Processing", *Procedia Computer Science*, 48, 735-740, 2015.
- [13] T. Lee, V. Ng, R. Gallagher, A. Coldman, D. McLean, "Dullrazor: A Software Approach to Hair Removal from Images", *Computers in biology and medicine*, 27(6), 533-543, 1997.
- [14] H. El-Khatib, D. Popescu, L. Ichim, "Deep Learning-Based Methods for Automatic Diagnosis of Skin Lesions", *Sensors Journal*, 20(6), 1-25, 2020.
- [15] K. Zafar, S. O. Gilani, A. Waris, A. Ahmed, M. Jamil, M. A. Khan, A. S. Kaskif, "Skin Lesion Segmentation from Dermoscopic Images Using Convolutional Neural Network", *Sensors Journal* 2020; 20(6). DOI: 10.3390/s20061601.
- [16] Celebi, E.C., Aslandoğan, A.A., Stoecker WV, Iyatomi H, Oka H, et al. "Unsupervised Border Detection in Dermoscopy Image", *Skin Research and Technology*, 13(4), 454-462, 2007.
- [17] D. N. H. Thanh, N. H. Hai, P. Tiwari, H. L. Minh, "Skin lesion segmentation method for dermoscopic images with convolutional neural networks and semantic segmentation", *Computer Optics*, 120, 121-129, 2021.
- [18] C. Akyel, N. Arıcı, "A New Approach to Hair Noise Cleaning and Lesion Segmentation in Images of Skin Cancer", *Journal of Polytechnic*, 23(3), 821-828, 2020.
- [19] N. Şahin, N. Alpaslan, "SegNet Mimarisi Kullanılarak Cilt Lezyon Bölütleme Performansının İyileştirilmesi", *Avrupa Bilim ve Teknoloji Dergisi*, Özel Sayı, 40-45, 2020.
- [20] Brahmhatt1, P., Rajan, S. N. "Skin Lesion Segmentation using SegNet with Binary CrossEntropy", **International Conference on Artificial Intelligence and Speech Technology (AIST2019)**, 14-15th November 2019.
- [21] L. Talavera-Martínez, P. Bibiloni and M. González-Hidalgo, "Hair Segmentation and Removal in Dermoscopic Images Using Deep Learning", in *IEEE Access*, 9, 2694-2704, 2021.
- [22] L. Wei, N.J.R. Alex, T. Tardi, Z. Zhemin, "Digital hair removal by deep learning for skin lesion segmentation", *Pattern Recognition*, 117, 1-15, 2021.
- [23] K. Polat, A. S. Ashour, Y. Guo, E. Kucukkulahli, P. Erdogmus, "A hybrid dermoscopy images segmentation approach based on neutrosophic clustering and histogram estimation", *Applied Soft Computing* 69, 426-434, 2018.
- [24] Abdulhamid, M., Sahiner, A., Rahebi, J. "New Auxiliary Function with Properties in Nonsmooth Global Optimization for Melanoma Skin Cancer Segmentation", *Hindawi BioMed Research International*, 1, 2020.
- [25] K.Hasan, L. Dahal, P. N. Samarakoon, F. I. Tushara, R. Marti, "DSNet: Automatic Dermoscopic Skin Lesion Segmentation", *Computers in biology and medicine*, 120, 426-434, 2020.
- [26] Internet: Stanford University, [https://web.stanford.edu/~kalouche/docs/Vision_Based_Classification_of_Skin_Cancer_using_Deep_Learning_\(Kalouche\).pdf](https://web.stanford.edu/~kalouche/docs/Vision_Based_Classification_of_Skin_Cancer_using_Deep_Learning_(Kalouche).pdf), 03.01. 2021.
- [27] C. Akyel, N. Arıcı, "LinkNet-B7: Noise Removal and Lesion Segmentation in Images of Skin Cancer", *Mathematics*, 736-751, 2022.
- [28] Internet: Task 3: LesionDiagnosis: Training, <https://challenge2018.isicarchive.com/task3/training/>, 20.10.2019.
- [29] Internet: ISIC 2018: Skin Lesion Analysis Towards Melanoma Detection, <https://challenge2018.isic-archive.com/>, 15.10.2019.
- [30] Internet: PH2 Dataset, <https://www.fc.up.pt/addi/ph2%20database.html>, 03.12.2021.
- [31] Internet: Arxiv, <https://arxiv.org/pdf/1411.4038.pdf>, 10.05.2021.
- [32] A. R. L'opez, S. Che, **Skin Lesion Detection From Dermoscopic Images Using Convolutional Neural Networks**, A Degree Thesis, Polytechnic University of Catalonia, Barcelona, Spain, 2017.
- [33] Internet: Softmax, <https://towardsdatascience.com/additive-margin-softmax-loss-am-softmax-912e11ce1c6b#:~:text=In%20short%2C%20Softmax%20Loss%20is,negative%20logarithm%20of%20the%20probabilities> 20.03.2022.
- [34] Internet: Keras, <https://keras.io/api/optimizers/adam/> 25.12.2021.
- [35] Y. Wang, A. Rahman, "Optimizing Intersection-Over-Union in Deep Neural Networks for Image Segmentation", **Conference: International Symposium on Visual Computing**, 10 December 2016.
- [36] T. Phan, S. Kim, H. Yang, G. Lee, "Skin Lesion Segmentation by U-Net with Adaptive Skip Connection and Structural Awareness", *Applied sciences*, 11(4528), 1-14, 2021.
- [37] F. Bagheri, M. J. Tarokh, M. Ziaratban, "Skin lesion segmentation based on mask RCNN, Multi Atrous Full-CNN, and a geodesic method", *Int J Imaging Syst Technol*, 31(3), 1609–1624, 2021.
- [38] C. K. Roy, J. R. Cordy, and R. Koschke. "Comparison and Evaluation of Code Clone Detection Techniques and Tools: A Qualitative Approach", *Sci. Comput. Program.*, 74(7), 470–495, 2009.